OPTICAL
PROPERTIES

Luminescence Properties of Solid Solutions of Borates Doped with Rare-Earth Ions

V. S. Levushkina[a, b, *], **V. V. Mikhailin**[a, c, †], **D. A. Spassky**[b, c],
B. I. Zadneprovski[d], **and M. S. Tret'yakova**[d]

[a] Moscow State University, Moscow, 119991 Russia
* e-mail: bestpum@mail.ru
[b] Institute of Physics, University of Tartu, Ülikooli 18, Tartu, 50090 Estonia
[c] Skobeltsyn Institute of Nuclear Physics, Moscow State University, Moscow, 119991 Russia
[d] Central Scientific Research Institute of Chemistry and Mechanics, ul. Nagatinskaya 16A, Moscow, 115487 Russia
Received December 30, 2013; in final form, April 29, 2014

Abstract—The structural and luminescence properties of $Lu_xY_{1-x}BO_3$ solid solutions doped with Ce^{3+} or Eu^{+3} have been investigated. It has been found that the solid solutions crystallize in the vaterite phase with a lutetium concentration $x < 0.5$. For a higher lutetium concentration x, the solid solutions contain an additional calcite phase with a content less than 5 wt %. The luminescence spectra are characterized by intensive impurity emission under excitation with the synchrotron radiation in the X-ray and ultraviolet spectral ranges. It has been shown that, as the lutetium concentration x in the $Lu_xY_{1-x}BO_3 : Ce^{3+}$ solid solutions increases, the emission intensity smoothly decreases, which is associated with a gradual shift of the Ce^{3+} $5d(1)$ level toward the bottom of the conduction band, as well as with a decrease in the band gap. It has been established that, in the $Lu_xY_{1-x}BO_3 : Eu^{3+}$ solid solutions with intermediate concentrations x, the efficiency of energy transfer to luminescence centers increases. This effect is explained by the limited spatial separation of electrons and holes in the solid solutions. It has been demonstrated that the calcite phase adversely affects the luminescence properties of the solid solutions.

DOI: 10.1134/S1063783414110171

1. INTRODUCTION

Complex inorganic compounds based on oxides have been widely used in various fields. In particular, borate compounds doped with rare-earth (*RE*) elements exhibit a high-intensity luminescence [1]. These compounds can be used in scintillation detectors, fluorescent tubes, and plasma displays. For example, europium-doped borates $(Y,Gd)BO_3 : Eu^{3+}$ have found use in plasma display panels owing to the effective conversion of ultraviolet (UV) radiation into visible light [2, 3]. Cerium-doped borates $Li_6RE(BO_3)_3 : Ce$ (RE = Gd, Y, Lu) have been used in neutron detectors intended for security systems [4]. The $LuBO_3 : Ce$ borate is a promising material for the use in scintillation detectors [5–9]. Interest expressed in this compound is caused by a unique combination of characteristics, such as the high density of the crystal ($\rho \sim 7.2$ g/cm^3) due to the presence of lutetium in the material, good radiation resistance, high light yield (up to 30000 photons/MeV), and fast scintillation decay ($\tau \sim 10^{-8}$ s) [5]. A significant disadvantage of lutetium borate is that it can crystallize in two phases (calcite and vaterite). The transition between these phases during cooling of the grown crystal inhibits the

growth of large-sized single crystals [6]. Nonetheless, in a number of papers, the authors proposed different methods for using polycrystalline lutetium borate in the detection of high-energy radiation (for example, in the form of scintillation films [7–9]). A possible method to solve the problem of growth of borate single crystals is a partial replacement of the lutetium cation by another isovalent cation. For example, in [5, 10], it was shown that the introduction of the scandium cation into the composition of lutetium borate provides the formation of single-phase $Lu_xSc_{1-x}BO_3$ solid solutions with the calcite structure type, which can already be grown in the form of bulk single crystals.

Another interesting feature of the solid solution is the possibility of increasing the efficiency of excitation energy transfer to luminescence centers, which leads to an increase in the scintillation light yield. An increase in the light yield was previously observed for solid solutions of perovskites $Lu_xY_{1-x}AlO_3 : Ce^{3+}$ [11, 12], borates $Lu_{1-x}Sc_xBO_3 : Ce^{3+}$ [13], silicates $(Lu,Gd)_2SiO_5 : Ce^{3+}$ [14], and garnets $Y_3(Al_{1-x}Ga_x)_5O_{12} : Ce^{3+}$ [15]. According to [11, 12], an increase in the light yield can be caused by the formation of clusters, i.e., regions with a predominant content of one of the components constituting the solid solution. This leads to a limited spatial separation

† Deceased.

of genetic electron–hole pairs formed upon absorption of photons of exciting radiation if the length of their diffusion is comparable to the cluster size.

In this work, we have performed the experimental investigation of the structural and luminescence properties of borate solid solutions $Lu_xY_{1-x}BO_3$ ($x = 0$, 0.25, 0.50, 0.75, 1.00) depending on the cation composition and the presence of Ce^{3+} and Eu^{3+} dopants in the compounds. Particular attention has been paid to the processes of band-to-band excitation energy transfer to impurity luminescence centers and their possible modification in the solid solutions because of the limited spatial separation of electrons and holes.

2. EXPERIMENTAL TECHNIQUE AND SAMPLE PREPARATION

The spectroscopic investigations of the $Lu_xY_{1-x}BO_3 : RE^{3+}$ ($RE = $ Ce, Eu) borate solid solutions were performed on experimental facilities providing measurements over a wide range of excitation energies.

The luminescence and luminescence excitation spectra, luminescence decay kinetics, and thermally stimulated luminescence (TSL) curves under excitation in the energy range from 3.7 to 22 eV were measured at the SUPERLUMI experimental station using synchrotron radiation (DESY, Hamburg, Germany) [16]. The samples were placed in a helium flow optical cryostat providing measurements over a wide temperature range from 4.2 to 400 K. The time-resolved luminescence spectra were recorded in the time intervals from 7 to 20 ns (TI1) and from 125 to 150 ns (TI2) with respect to the maximum of the synchrotron radiation excitation pulse. The time intervals were chosen taking into account the time of Ce^{3+} luminescence decay in the matrix of borates so as to separate the "fast" processes caused by the relaxation of bound electron–hole pairs (intracenter transitions or energy transfer from excitons) at the Ce^{3+} centers and the "slow" processes associated with the intermediate stages of transfer of spatially separated electron–hole pairs to the Ce^{3+} centers. The TSL curves were measured after irradiation of the samples at a temperature of 10 K for 20 min. The irradiation was performed by synchrotron radiation in the vacuum ultraviolet (VUV) range with an energy of 14 eV. After the irradiation, the sample was heated at a constant rate of 10 K/min.

The luminescence and luminescence excitation spectra were measured in the UV and visible ranges on a facility based on the LOT-Oriel MS-257 spectrograph at the Department of Physical Problems of Quantum Electronics of the Skobeltsyn Institute of Nuclear Physics, Moscow State University (Russia). This facility permitted measurements of luminescence spectra in the range of 300–1050 nm and luminescence excitation spectra in the range of 220–500 nm at

temperatures in the range of 80–350 K [17]. The luminescence spectra were normalized to the function of the instrumental sensitivity of the detection system for all the aforementioned facilities.

The luminescence measurements under excitation in the soft X-ray range (130 eV) were performed on a facility installed at the BW3 undulator-radiation beamline at the DORIS III storage ring. The secondary monochromator of the facility was optimized for the UV spectral region, and the rotation angle of the diffraction grating of the monochromator permitted measurements of the luminescence spectra in the range from 110 to 500 nm. The excitation photon flux density at the sample reached 10^{12} photons/s [18]. The luminescence spectra were not normalized to the function of the instrumental sensitivity of the detection system of the facility installed at the BW3 beamline. The measurements were carried out in the temperature range from 10 to 300 K. The measurements of luminescence spectra of $Lu_xY_{1-x}BO_3 : Eu^{3+}$ with the use of an X-ray source with a tungsten anode at $U = 30$ keV were performed at the Laboratory of Physical Chemistry of Luminescent Materials of the Claude Bernard University Lyon.

The X-ray diffraction patterns ($\lambda = 1.5405$ Å) of the samples were recorded on a Rigaku Ultima IV X-ray diffractometer.

Series of borate solid solutions $Lu_xY_{1-x}BO_3$ ($x = 0$, 0.25, 0.50, 0.75, 1.00) doped with 1 mol % Ce^{3+} or 1 mol % Eu^{3+} were synthesized by the sol–gel method at the Mendeleev Central Research Institute of Chemistry and Mechanics. The synthesis was performed in several stages, which included the transfer of water-insoluble oxides into a solution, the preparation of a reaction mixture containing rare-earth elements and a dissolved form of boric acid, and the precipitation of the product. The final stage included crystallization of the synthesized material. For this purpose, the sample was subjected to high-temperature annealing under the following conditions: the annealing temperature was 960°C, the exposure time was 2 h, and the atmosphere was air. The synthesis procedure was described in more detail in [19]. According to the granulometric analysis, the dominant size of particles for all the compositions was ~500 nm.

3. EXPERIMENTAL RESULTS

3.1. Investigations of the Structure of Borate Solid Solutions

As follows from the X-ray powder diffraction data, the synthesized compound is a well-structured lutetium borate without intermediate phases; however, the samples containing less than 50% yttrium include two structurally different phases isostructural with the phases of calcite and vaterite (Table 1). In all samples, the vaterite phase dominates. The calcite phase is

found in $Lu_xY_{1-x}BO_3 : Ce^{3+}$ with a lutetium concentration $x \geq 0.5$ and in $Lu_xY_{1-x}BO_3 : Eu^{3+}$ with $x \geq 0.75$. The content of the calcite phase increases with an increase in the lutetium concentration in the solid solution but does not exceed 5 wt % (Fig. 1).

The results of the determination of the unit cell parameters showed that, upon transition from the two-phase composition to the single-phase composition, the dependences of the lattice parameters a and c and the unit cell volume V on the concentration ratio of lutetium and yttrium cations have a kink for the $Lu_{0.50}Y_{0.50}BO_3$ composition. This can indicate that the presence of the calcite phase in the compound affects the unit cell parameters of the vaterite phase.

3.2. Luminescence Properties of Europium-Doped Borates

The luminescence spectra of the series of $Lu_xY_{1-x}BO_3 : Eu^{3+}$ solid solutions are shown in Fig. 2 for the sample with $x = 0.75$ taken as an example. Using the selective excitation, we obtained luminescence spectra that are characteristic of all samples of the series (Fig. 2, curve 1), as well as of the samples with the calcite phase (Fig. 2, curve 2). The luminescence observed in the form of narrow lines is typical of the compounds doped with Eu^{3+} and corresponds to the intracenter $f–f$ electron transitions in the europium ion. All the bands observed in the luminescence spectrum can be assigned to the intracenter transitions $^5D_0–^7F_j$ ($j = 0, 1, 2, 3, 4$) in the Eu^{3+} ion. The spectrum typical of all samples of the series is most likely associated with the Eu^{3+} emission in lutetium borate, which crystallizes in the vaterite structure type, and agrees with the previously obtained data [19]. The structure of the additional Eu^{3+} luminescence spectrum observed in the samples with the calcite phase differs significantly from the structure typical of the vaterite phase due to different symmetries of the Eu^{3+} environments. Probably, the presence of the calcite phase in the sample leads to the fact that a part of the Eu^{3+} ions occupy lattice sites whose environment has the symmetry distorted by the closely located calcite phase. In this case, the spectrum cannot be assigned to the emission of Eu^{3+} ions located directly in the calcite phase. According to [19], this spectrum is characterized by the presence of only two lines in the region of 590 nm, whereas the observed spectrum contains a larger number of bands.

The relative intensity of the luminescence spectra measured for the series of $Lu_xY_{1-x}BO_3 : Eu^{3+}$ solid solutions under VUV and X-ray excitations was obtained by integrating over the luminescence spectrum in the range of 570−720 nm (Fig. 2). The VUV excitation energy (11 eV) exceeds the band gap of the considered borates. The maximum intensity was observed in the solid solutions with intermediate rela-

Table 1. Parameters of the crystal structure of the phases isostructural with vaterite and calcite for $Lu_xY_{1-x}BO_3 : RE^{3+}$ (RE = Ce, Eu)

x	Vaterite			Calcite		
	a, Å	c, Å	V, Å³	a, Å	c, Å	V, Å³
			Ce			
1.00	3.736	8.707	105.27	4.914	16.233	339.4
0.75	3.739	8.733	105.78	4.920	16.277	341.2
0.50	3.747	8.752	106.46	4.934	16.293	343.5
0.25	3.762	8.780	107.66	–	–	–
0	3.774	8.797	108.54	–	–	–
			Eu			
1.00	3.732	8.715	105.13	4.914	16.23	339.5
0.75	3.745	8.726	105.96	4.92	16.32	342.2
0.50	3.748	8.755	106.52	–	–	–
0.25	3.761	8.778	107.52	–	–	–
0	3.777	8.804	108.80	–	–	–

tive concentrations of cations. For example, the maximum intensity is reached in the solid solution with $x = 0.5$ for VUV excitation and in the solid solution with $x = 0.25$ for X-ray excitation. As the single-cation
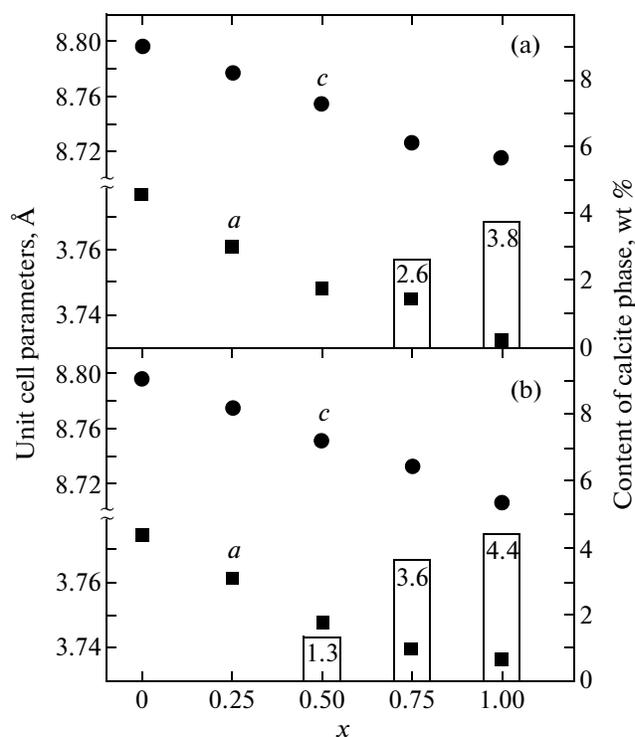

Fig. 1. Dependences of the unit cell parameters a (squares) and c (circles) and the content of calcite phase (bars) in (a) $Lu_xY_{1-x}BO_3 : Eu^{3+}$ and (b) $Lu_xY_{1-x}BO_3 : Ce^{3+}$ on the lutetium concentration x.

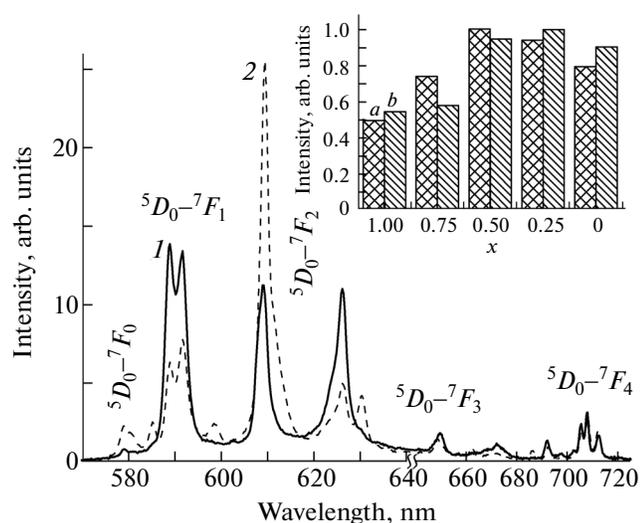**Fig. 2.** Luminescence spectra of the $Lu_{0.75}Y_{0.25}BO_3 : Eu^{3+}$ solid solution at excitation energies $E_{ex} = (1)$ 5.4, and (2) 5.9 eV. $T = 300$ K. The inset shows the relative intensity of the luminescence spectra of the $Lu_xY_{1-x}BO_3 : Eu^{3+}$ solid solutions for (a) excitation energy $E_{ex} = 11$ eV and (b) X-ray excitation at 30 keV.

composition of the borate is approached, the luminescence intensity gradually decreases.

The luminescence excitation spectra of $Lu_xY_{1-x}BO_3 : Eu^{3+}$ are shown in Fig. 3. In the range from 2.5 to 4.5 eV (Fig. 3a), there is a series of narrow low-intensity bands that are characteristic of the intracenter $f–f$ transitions in the Eu^{3+} ion. The most intense peaks are attributed to the transitions $^7F_0–^5D_2$, $^7F_0–^5L_6$, $^7F_0–^5D_4$, and $^7F_0–^5H_j$ in the Eu^{3+} ion. The position and relative intensity of peaks in this range do not depend on a particular sample. This indirectly confirms that the europium concentrations are equal to each other. Since the electron transitions between different terms of the f shell are forbidden in the dipole approximation, the intensity of the bands is relatively low. In the range from 4.5 to 7.0 eV, there is an intense broad non-elementary peak due to the luminescence excitation in the band with charge transfer from oxygen to europium (Fig. 3b). The intensity of this peak is approximately two orders of magnitude higher than the intensity of narrow bands in the low-energy range.

A further increase in the excitation energy leads to the appearance of two overlapping bands with maxima at 7.25 and 7.76 eV. The position of the peak at 7.76 eV coincides with the first peak in the luminescence excitation spectrum of self-trapped exciton emission in undoped yttrium borate (Fig. 3b). This peak can be used to estimate the position of the fundamental absorption edge. The band with the maximum at 7.25 eV lies in the region before the fundamental absorption edge and can be attributed to the intrac-

enter $4f–5d$ transition in the Eu^{3+} ion. Usually, the energy of these transitions in the Eu^{3+} ion is higher than the energy of the electron transitions in the charge-transfer band. According to [20, 21], the $f–d$ transitions in the Eu^{3+} ion are observed in some of phosphates and in yttrium oxide in the range of 8.2–8.5 eV. The energy position of the $5d$ level depends strongly on the matrix doped with Eu^{3+}. Therefore, we can expect that this level in borates will be shifted by 1 eV toward the low-energy range with respect to its position in phosphates and yttrium oxide.

With a further increase in the excitation energy ($E_{ex} > 8$ eV), the luminescence excitation spectra exhibit band-to-band transitions. The region of band-to-band transitions was more precisely determined using time-resolved spectroscopy for Ce^{3+}-doped solid solutions. In this energy range, the formation of luminescence excitation spectra can occur in two ways, namely, through the exciton channel ($e + h–ex–Eu^{3+(*)}–Eu^{3+} + h\nu$) and the recombination channel ($Eu^{3+} + e–Eu^{2+} + h–Eu^{3+(*)}–Eu^{3+} + h\nu$) [23]. In the first case, the electron and hole are bound to form an exciton (ex), which falls on the luminescence center, followed by the emission of a photon. In the second case, the luminescence center first captures an electron and then a hole, followed by the emission. The peak observed in the fundamental absorption edge region (~7.5 eV) in the luminescence excitation spectra is characteristic of the exciton-type energy transfer to luminescence centers. However, a further decrease in the luminescence intensity after this peak is not observed, which usually occurs in the case of energy transfer to Eu^{3+} exclusively through the exciton channel. With a further increase in the excitation energy $E_{ex} > 8$ eV, the luminescence intensity gradually increases, which is characteristic of the recombination energy transfer to luminescence centers. Therefore, it can be assumed that, in our case, the contribution to the formation of the luminescence excitation spectrum of $Lu_xY_{1-x}BO_3 : Eu^{3+}$ comes from two main channels of energy transfer to luminescence centers, namely, the exciton and recombination channels.

3.3. Luminescence Properties of Cerium-Doped Borates

3.3.1. Luminescence spectra. The characteristic luminescence spectrum measured for the series of $Lu_xY_{1-x}BO_3 : Ce^{3+}$ borates under UV excitation is shown in Fig. 4. The luminescence is observed in the form of two bands with maxima at 380 and 420 nm (the main doublet), which are caused by the $5d–{}^7F_{5/2, 7/2}$ radiative transitions in the Ce^{3+} ion. The relative luminescence intensity gradually decreases with an increase in the lutetium concentration x (Fig. 4, inset). The maxima of the luminescence bands in this case shift to the long-wavelength range. This shift can
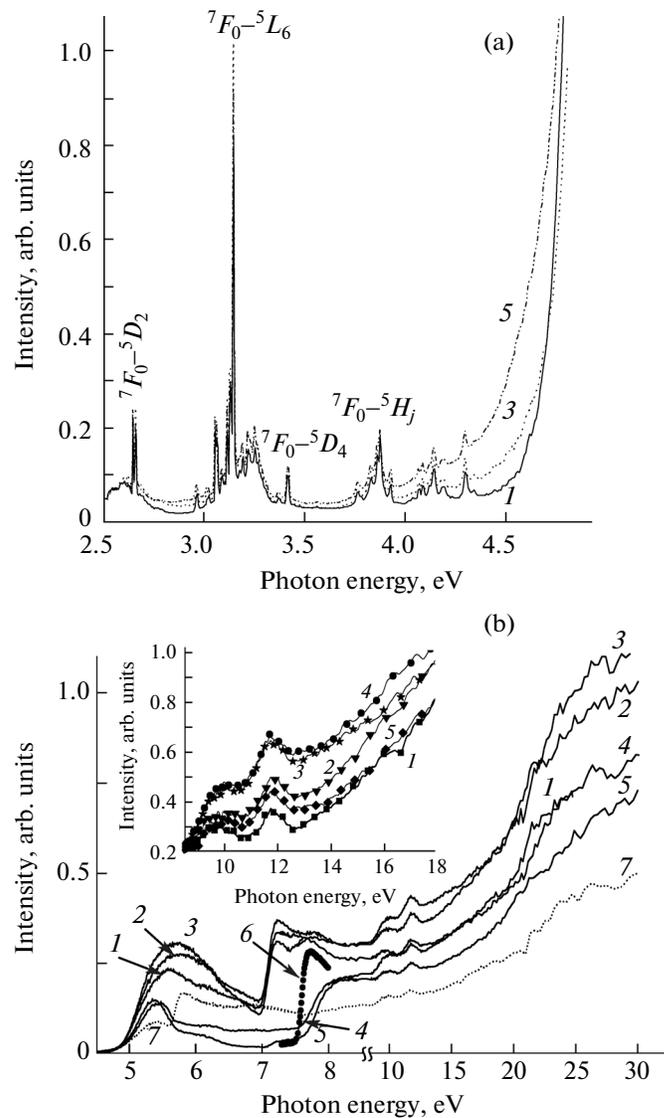
Fig. 3. Luminescence excitation spectra of the $Lu_xY_{1-x}BO_3 : Eu^{3+}$ solid solutions in the photon energy ranges of (a) 2.5–4.7 and (b) 4.5–30 eV. $\lambda_{em} = 590$ nm, $T = 300$ K. $x = $ (*1*) 0, (*2*) 0.25, (*3*) 0.50, (*4*) 0.75, and (*5*) 1.00. (*6*) Excitation spectrum of self-trapped exciton emission for undoped YBO_3 at $\lambda_{em} = 260$ nm and $T = 10$ K. (*7*) Luminescence excitation spectrum of $Lu_{0.75}Y_{0.25}BO_3 : Eu^{3+}$ at $\lambda_{em} = 610$ nm and $T = 300$ K. The inset shows the luminescence excitation spectra of $Lu_xY_{1-x}BO_3 : Eu^{3+}$. The spectra are normalized to the intensity at $E = 8.2$ eV.

be explained by an increase in the strength of the crystal field in the solid solution, which is associated with a decrease in the lattice parameter due to the gradual substitution of yttrium cation for the lutetium cation (Fig. 1). Indeed, the distance between the positively charged cation and the oxyanion group BO_4^{5-} decreases, which usually leads to an increase in strength of the crystal field [23].

The luminescence spectra of the solid solutions measured under soft X-ray excitation ($E_{ex} = 130$ eV), apart from the main doublet, contain an additional doublet with maxima at 315 and 344 nm, whose inten-

sity is lower by approximately one order of magnitude. The nature of this doublet will be discussed below.

3.3.2. Luminescence excitation spectra. The Ce^{3+} luminescence excitation spectra are shown in Fig. 5. In the energy range up to 7 eV, there are five peaks due to the intracenter excitation of the Ce^{3+} ion into the $5d(1)-5d(5)$ levels. In the luminescence excitation spectra, the observed splitting of the Ce^{3+} d levels into two low-energy and three high-energy levels is characteristic of the Ce^{3+} ion surrounded by eight ligands [24]. Earlier [25], based on the analysis of the luminescence excitation spectra, the assumption was made
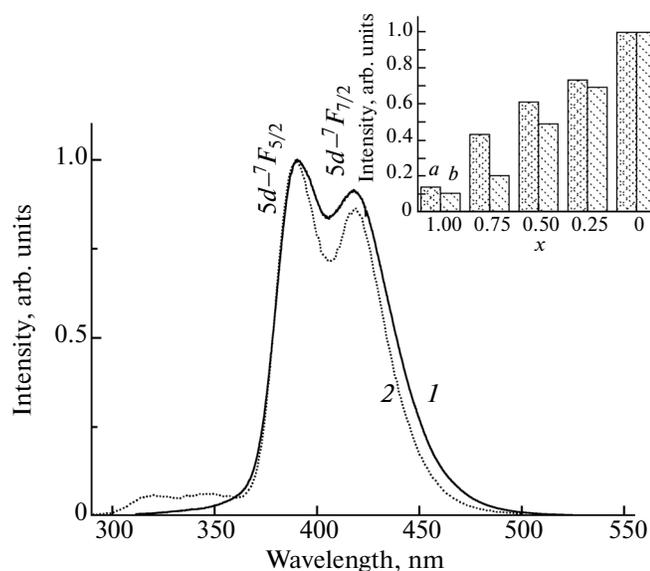
Fig. 4. Luminescence spectrum of the $Lu_{0.5}Y_{0.5}BO_3$: Ce^{3+} solid solution at excitation energies E_{ex} = (*1*) 11 and (*2*) 130 eV. $T = 300$ K. The inset shows the relative intensity of the luminescence spectra for the $Lu_xY_{1-x}BO_3$: Ce^{3+} solid solutions at E_{ex} = (a) 11 and (b) 130 eV.

about the splitting of the Ce^{3+} *d* levels into three low-energy and two high-energy levels in $LuBO_3$. In this case, the environment of the Ce^{3+} ion should have a symmetry close to octahedral (coordination number is 6). The exact type of the space group of the vaterite phase is still not determined. The coordination number of the cation substituted for by the Ce^{3+} ion, according to different authors, can be 6 or 8 [26–30]. At the same time, according to more recent data [30], the most probable space group for vaterite is $C2c$, in which the cation is surrounded by eight ligands. In this case, the *d* orbitals are split into two low-energy and three high-energy orbitals, as was observed in our experiments.

The excitation energies $E_{ex} > 7$ eV correspond to the fundamental absorption edge region. In this region, there can be both "fast" and "slow" processes of energy transfer to luminescence centers. The former processes are caused by the formation of excitons, whereas the latter processes correspond to the excitation of luminescence centers through the successive capture of a hole and an electron. The use of time-resolved spectroscopy allowed us to separate these processes in the fundamental absorption edge region (Fig. 5, inset). The peak at 7.6 eV is associated
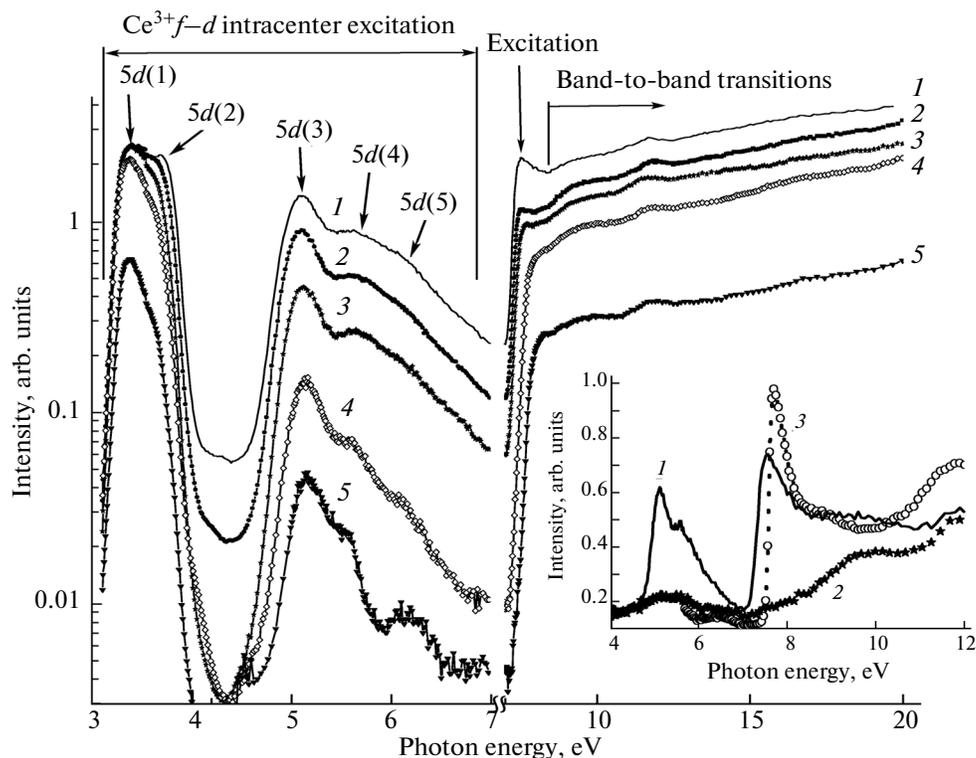

Fig. 5. Luminescence excitation spectra of the $Lu_xY_{1-x}BO_3$: Ce^{3+} solid solutions at x = (*1*) 0, (*2*) 0.25, (*3*) 0.50, (*4*) 0.75, and (*5*) 1.00. $\lambda_{em} = 420$ nm, $T = 300$ K. The inset shows the time-resolved luminescence excitation spectra of YBO_3 : Ce^{3+} measured in the time intervals (*1*) TI1 = 7–20 ns and (*2*) TI2 = 125–150 ns. $\lambda_{em} = 420$ nm, $T = 300$ K. (*3*) Excitation spectrum of self-trapped exciton emission in YBO_3 at $\lambda_{em} = 260$ nm and $T = 10$ K.

with the formation of an exciton in the fundamental absorption edge region. This peak is observed only in the time gate intervals TI1, and its position corresponds to the first peak of the excitation of self-trapped exciton emission in the undoped YBO_3 sample.

The onset of band-to-band transitions can be determined from the increase in intensity of the luminescence excitation spectrum measured in the time intervals TI2. In particular, for the $YBO_3 : Ce^{3+}$ borate, the threshold is observed at 8.2 eV (Fig. 5, inset). This value is an estimate of the band gap E_g. The estimated value of E_g is larger than the values (7.0–7.1 eV) obtained from theoretical calculations [31, 32]. However, the calculations usually give underestimated values of E_g. In the band-to-band excitation region, the energy transfer to luminescence centers is possible in two ways, namely, through the exciton channel ($e + h-$ $ex-Ce^{3+(*)}-Ce^{3+} + h\nu$) and the recombination channel ($Ce^{3+} + h-Ce^{4+} + e-Ce^{3+(*)}-Ce^{3+} + h\nu$). After analyzing the luminescence excitation spectra in the energy range under consideration, we concluded that the contribution to the formation of the luminescence excitation spectrum of $Lu_xY_{1-x}BO_3 : Ce^{3+}$ comes from both the exciton and recombination channels, as was observed in the system of borate solid solutions doped with europium.

3.3.3. Luminescence decay kinetics. Figure 6a shows the luminescence decay kinetics for the $Lu_{0.5}Y_{0.5}BO_3 : Ce^{3+}$ sample at three excitation energies: (i) at the energy of 5.2 eV, which corresponds to the Ce^{3+} intracenter excitation; (ii) at the energy of 8.0 eV, which corresponds to the fundamental absorption edge region with the possible formation of excitons; and (iii) at the energy of 11 eV, which corresponds to the region of band-to-band transitions. The characteristic luminescence decay times τ and the contributions to the decay kinetics of slower compo-
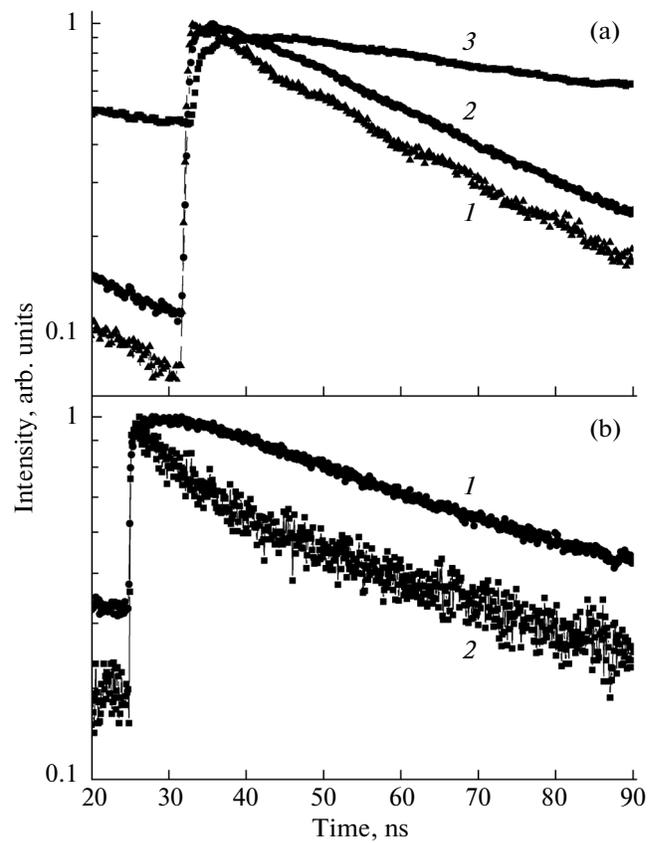

Fig. 6. Kinetics of luminescence decay in $Lu_{0.5}Y_{0.5}BO_3 :$ Ce^{3+} for (a) $E_{ex} = $ (*1*) 5.2, (*2*) 8.0, and (*3*) 11 eV, $\lambda_{em} = $ 380 nm, $T = 300$ K and (b) $E_{ex} = 130$ eV, $\lambda_{em} = $ (*1*) 380 and (*2*) 320 nm, $T = 300$ K.

nents y_0 for the studied series of solid solutions at different excitation energies are presented in Table 2.

The luminescence decay times for the intracenter excitation of the Ce^{3+} ion lie in the range of 22–30 ns

Table 2. Parameters of the luminescence decay kinetics for $Lu_xY_{1-x}BO_3 : Ce^{3+}$ solid solutions at different excitation energies (y_0 is the level of contribution to the luminescence decay kinetics from slow components, τ is the luminescence decay time in nanoseconds)

E_{ex}, eV	Parameter	x				
		0	0.25	0.50	0.75	1.00
5.2	τ	29.66	29.62	27.32	21.83	1.67/21.7*
	y_0	0.04	0.059	0.05	0.09	0.04
8.3	τ	36.53	39.45	36.06	38.16	31.57
	y_0	0.05	0.055	0.05	0.07	0.04
13.8	τ	43.65	67.09	58.29	50.42	31.29
	y_0	0.25	0.17	0.16	0.15	0.05
130	τ ($\lambda_{em} = 380$ nm)	33.43	–	53.01	32.25	19.27
	τ ($\lambda_{em} = 320$ nm)	3.17/33.4*	–	5.66/53.0*	6.86/32.3*	4.94/19.3*

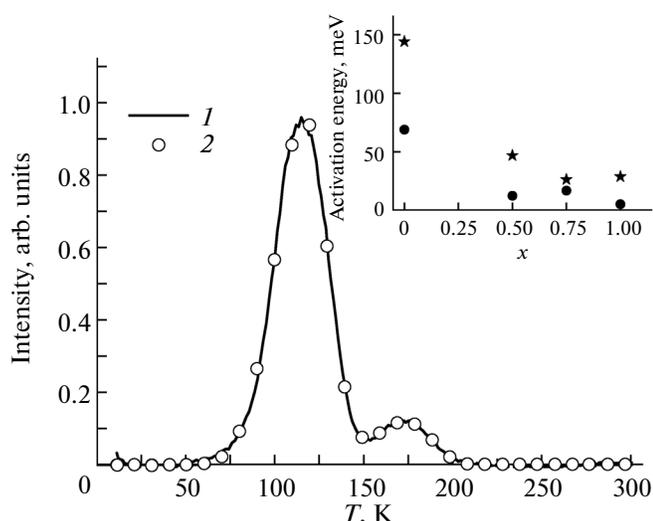* The decomposition of the luminescence decay kinetics was performed using two exponential functions.

Fig. 7. (*1*) TSL curve of $YBO_3 : Ce^{3+}$ and (*2*) fitting of the TSL curve in the first-order kinetic approximation. The inset shows the dependence of the activation energy of traps in $Lu_xY_{1-x}BO_3 : Ce^{3+}$ on the lutetium concentration *x*. Asterisks and circles indicate the activation energies of the traps corresponding to the high-temperature and low-temperature peaks of the TSL curve, respectively.

for all samples, except $LuBO_3 : Ce^{3+}$. The obtained luminescence time is characteristic of cerium-doped borates [25]. In the case of lutetium borate upon excitation in this region, the luminescence kinetics at the initial stage is fast and non-exponential. Presumably, this kinetics is associated with the quenching of the luminescence due to the presence of the calcite phase with the maximum content in the studied sample (Fig. 1).

The slowing down of the luminescence decay time upon excitation in the fundamental absorption edge region to $36-39$ ns can be explained by the fact that the energy transfer includes an additional intermediate stage associated with the formation of excitons. A further increase in the luminescence decay time upon excitation in the region of band-to-band transitions, as compared to the above-considered regions, is caused by the dominant formation of spatially separated $e-h$ pairs under the same conditions. An electron or a hole either can be sequentially captured by a cerium impurity center or can create an exciton with its subsequent capture by cerium. Moreover, the components of the pair can be trapped, which will delay the excitation transfer to luminescence centers. This can be responsible both for the observed buildup of luminescence and for the increased level of the contribution from the slower components y_0.

The luminescence decay kinetics measured upon high-energy excitation at 130 eV is shown in Fig. 6b. The luminescence decay curves measured at the initial stage in additional doublet bands ($\lambda_{em} = 320$ nm) differ significantly from the curves measured in the bands of the main doublet ($\lambda_{em} = 380$ nm). For the main doublet, the buildup of luminescence is observed at the initial stage, as is the case with the band-to-band excitation in the VUV range. The kinetics measured in the additional doublet band has no buildup at the initial stage, and the luminescence decay time is substantially shorter. It should be noted that the kinetics has a nonexponential behavior, and its approximation requires two exponential functions. In this case, the longer decay time corresponds to the luminescence decay time of the main doublet.

Apparently, the additional doublet is also associated with the Ce^{3+} luminescence. The distance between the maxima of the doublet corresponds to the splitting between the $^7F_{5/2}$ and $^7F_{7/2}$ terms of the Ce^{3+} ion. It should be noted that this doublet is observed only upon high-energy photon excitation, when radiation-induced defects are formed in borates. In particular, for undoped $Lu_xY_{1-x}BO_3$ samples, we previously showed that the intrinsic luminescence undergoes a significant degradation with time [33], which confirms the formation of defects in solid solutions at $E_{ex} = 130$ eV. We assume that the appearance of the additional doublet is caused by a modification of the symmetry of the cerium environment due to the formation of radiation-induced defects. The possibility of the appearance of additional Ce^{3+} luminescence bands under high-energy radiation was shown earlier for sulfides [34]. The formation of radiation-induced defects (for example, oxygen vacancies) leads to a change in the crystal field in the cerium environment, which causes a shift of the *d* levels and, consequently, a shift of the bands in the luminescence spectrum. This is further followed by the rapid "healing" of the defects (for example, oxygen returns to its site). As a result of this sequence of processes, first, a rapid (unusual for this series of solid solutions) cerium emission is observed in the luminescence band at 320 nm, but then, within ~20 ns after the excitation radiation pulse, the defect is healed, and a characteristic decay kinetics of the main doublet is observed in the interval of $30-50$ ns at its short-wavelength edge.

3.3.4. Thermally stimulated luminescence curves. The presence of traps in the band gap, as a rule, adversely affects the scintillation properties of the crystals of the samples. However, their investigation for series of solid solutions provides important information on the shift of the electronic states of the energy bands in the region of the conduction band bottom or the valence band top [35]. The TSL characteristic curve for $YBO_3 : Ce^{3+}$ is shown in Fig. 7. During heating, the TSL curve exhibits two peaks with maxima at 115 and 174 K. For other samples of the series, there are also two broad bands, whose intensity decreases with an increase in the concentration *x*, and the TSL peaks shift to the low-temperature range.

The TSL curves were fitted in the first-order kinetic approximation, according to which free charge carriers, with a higher probability, are bound into an exciton, rather than are trapped. In this approximation, the elementary peak is described by the formula

$$I_l = n(0)\omega_0\exp\left(-\frac{E_A}{k_B T(t)}\right.$$
$$\left. - \frac{\omega_0 k_B T^2(t)}{E_A T'(t)}\exp(-E_a/k_B T(t))\right),$$

where $n(0)$ is the concentration of traps, ω_0 is the frequency factor, E_A is the activation energy, $T(t)$ is the temperature of the sample, and $T'(t)$ is the heating rate (in this case, the heating rate was constant and equal to 10 K/min) [22]. The experimental TSL curves are characterized by two well-defined peaks, so that the result of the fitting is represented by the sum of two elementary peaks. It can be seen from Fig. 7 that, in the first-order kinetic approximation under the assumption of the existence of two types of traps with different activation energies, the result of the fitting adequately describes the experimental TSL curve. The performed fitting ignores the possible interaction between traps of different types. The profile of each of the experimental peaks can be satisfactorily fitted using only one set of parameters including the trap activation energy E_A. The dependence of the activation energy of traps on the lutetium concentration x in the solid solution is shown in the inset to Fig. 7.

3.4. Analysis of the Change in the Efficiency of Energy Transfer to Luminescence Centers in Series of Solid Solutions $Lu_xY_{1-x}BO_3 : Eu^{3+}$ and $Lu_xY_{1-x}BO_3 : Ce^{3+}$

3.4.1. Series of solid solutions $Lu_xY_{1-x}BO_3 : Eu^{3+}$. The observed effect of increase in the intensity of luminescence in the series of $Lu_xY_{1-x}BO_3 : Eu^{3+}$ solid solutions with intermediate values of x can be explained by the limited spatial separation between genetic electrons and holes. This leads to an increase in the probability that an electron and a hole will be trapped into a luminescence center through the successive capture or through preliminary formation of an exciton. This limitation can be associated, for example, with the clustering of the solid solution, as was assumed earlier in [11, 12]. However, the analysis of the results should take into account the effect exerted by the formation of the calcite phase in solid solutions. The presence of the calcite phase in the solid solution leads to the formation of a competing radiative channel of relaxation. The excitation spectra of the Eu^{3+} luminescence, which is characteristic of the vaterite phase, and the excitation spectra of the luminescence of Eu^{3+} ions, which occupy lattice sites whose environment has the symmetry distorted by the closely

located calcite phase (Fig. 3b, curve 7), indicate a competition between these luminescence centers. For example, the peaks at 7.25 and 7.76 eV almost completely disappear in the samples containing the calcite phase (Fig. 3b). In this case, the Eu^{3+} luminescence in lattice sites whose environment has the symmetry distorted by the closely located calcite phase is effectively excited in the range of 5.5–8.0 eV. The presence of the calcite phase in the solid solution can lead not only to the formation of a competing radiative channel but also to the formation of a nonradiative channel of energy relaxation. Therefore, it is necessary to take into account that a decrease in the integrated intensity of luminescence in the samples with $x = 0.75$ and 1.00 can be associated not only with the manifestation of the effect of the limited spatial separation of electrons and holes but also with the adverse influence of the presence of the calcite phase in the samples. Nonetheless, the results presented below suggest that the efficiency of energy transfer increases in the samples with intermediate concentrations x.

For more information and convenience of the analysis of the processes of energy transfer to luminescence centers, all the luminescence excitation spectra of the solid solutions under investigation were normalized to the energy of 8.2 eV, which corresponds to the onset of band-to-band transitions (Fig. 3b, inset). The slope of the spectra allows us to judge about the efficiency of band-to-band excitation energy transfer to luminescence centers. As can be seen from the inset in Fig. 3b, the efficiency of energy transfer upon band-to-band excitation increases for samples of solid solutions with $x = 0.25$, 0.50, and 0.75 as compared to the extreme compositions ($x = 0$ and 1). The revealed effect confirms the assumption on the limited spatial separation of genetic electrons and holes in solid solutions. It should be noted that the maximum increase in the efficiency is observed for the sample with $x = 0.75$. It is for this sample that we could expect the highest luminescence intensity. However, the presence of the calcite phase in the solid solution leads to the formation of additional energy relaxation channels. As a result, no increase in the luminescence intensity is observed in the region of band-to-band transitions for this sample as compared to the samples with $x = 0.25$ and 0.50.

3.4.2. Series of solid solutions $Lu_xY_{1-x}BO_3 : Ce^{3+}$. In the series of $Lu_xY_{1-x}BO_3 : Ce^{3+}$ solid solutions, the luminescence intensity gradually decreases with an increase in the lutetium concentration x for all excitation energies, except for $E_{ex} = 3.4$ eV, which corresponds to the Ce^{3+} intracenter excitation through the $5d(1)$ level. The luminescence intensity at $E_{ex} = 3.4$ eV remains constant for the samples with $x = 0$, 0.25, and 0.50 and decreases with an increase in the lutetium concentration beginning with $x = 0.75$ (Fig. 5). This behavior can also be explained by the influence of the calcite phase which forms competing energy relaxation
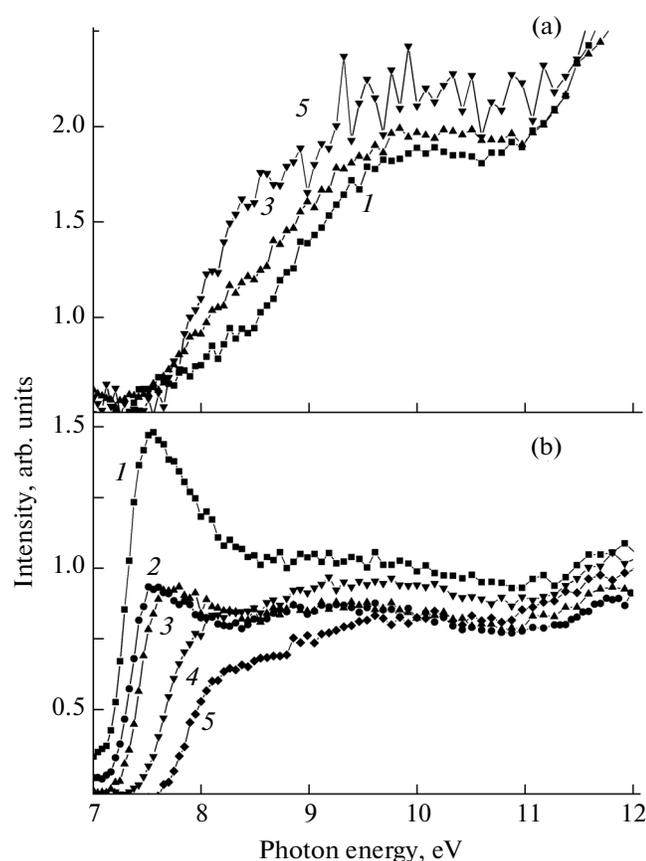
Fig. 8. Time-resolved luminescence excitation spectra of the $Lu_xY_{1-x}BO_3 : Ce^{3+}$ solid solutions with x = (*1*) 0, (*2*) 0.25, (*3*) 0.50, (*4*) 0.75, and (*5*) 1.00 in the time intervals (a) TI2 = 125−150 ns and (b) TI1 = 7−20 ns, λ_{em} = 420 nm, T = 300 K.

channels. However, in the case of $Lu_xY_{1-x}BO_3 : Ce^{3+}$, the competitive role of the calcite phase is not obvious. The intensity of the first band changes only beginning with x = 0.75, whereas the calcite phase is observed already for x = 0.5. Moreover, there are no additional luminescence bands of Ce^{3+} ions that occupy lattice sites whose environment has the symmetry distorted by the closely located calcite phase, as was observed in the case of $Lu_xY_{1-x}BO_3 : Eu^{3+}$.

Another assumption, which can explain the observed effect, is a gradual shift of the Ce^{3+} d levels toward the bottom of the conduction band with a gradual increase in the value of x. This shift can be caused by a narrowing of the band gap, as well as by a shift of the d levels toward the high-energy range. The experimental TSL data and time-resolved luminescence excitation spectra evidence in favor of the narrowing of the band gap with an increase in the lutetium concentration x.

The TSL peaks are shifted to the low-temperature range, which leads to a decrease in the activation energy of traps with an increase in the concentration x

(Fig. 7, inset). It is known that the cerium luminescence center captures first a hole and only then an electron. Therefore, the analysis of the TSL curves in Ce^{3+} luminescence bands provides information about changes in the parameters of electron traps [35]. The observed decrease in the activation energy of traps with an increase in the value of x indicates a shift of the conduction band bottom toward the low-energy range.

The time-resolved luminescence excitation spectra also indicate that the band gap E_g decreases with an increase in x. The change in the band gap can be determined from the analysis of the luminescence excitation spectra measured in the time intervals TI2. Figure 8 shows the time-resolved spectra for the series of solid solutions doped with Ce^{3+}. The observed shift of the fundamental absorption edge toward the low-energy range with an increase in the Lu concentration suggests a gradual decrease in the band gap (Fig. 8a). It should be noted that an attempt to analyze the shift of the fundamental absorption edge in the luminescence excitation spectra measured in the time intervals IT1 can lead to an opposite conclusion (Fig. 8b). Indeed, in this case, the threshold shifts to the high-energy range with an increase in x. The spectra measured in the time intervals TI1 allow us to detect an exciton peak at the fundamental absorption edge. Thus, it can be concluded that the formation of excitons is gradually suppressed with an increase in x. In our recent work [33], for undoped borates it was shown that, in borates with the vaterite phase, excitons are generated with the participation of cationic states that form the bottom of the conduction band. A gradual substitution of yttrium cations, the states of which form a separate narrow subband in the region of the conduction band bottom, for lutetium cations with a significantly greater dispersion of states in the region of the conduction band bottom [31] can decrease the probability of the formation of excitons. This conclusion is consistent with the decrease in the intensity of self-trapped exciton emission in undoped borates with an increase in x [33]. In the series of solid solutions with an increase in the lutetium concentration beginning with x = 0.75, the contribution of the fast component significantly decreases in the region of the exciton peak at 7.5 eV and completely disappears for $LuBO_3$, which can be associated with an additional adverse influence on the formation of an exciton in the calcite phase. According to the calculations [31], the bottom of the conduction band in the calcite phase is formed by the boron states, which have an adverse effect on the localization of hot electrons.

It should be noted that, although there is no manifestation of the possible effect of clustering of the solid solution in the luminescence spectra, we obtained indirect evidence of its manifestation in the series of $Lu_xY_{1-x}BO_3 : Ce^{3+}$ solid solutions. According to the data presented in Table 2, the luminescence decay

times increase for intermediate values of x in solid solutions under band-to-band excitation. Indeed, the cluster boundaries are characterized by a high concentration of defects that limit the rate of excitation transfer to Ce^{3+} ions. This should lead to an increase in the luminescence decay time, which was observed in the experiment.

4. CONCLUSIONS

The luminescence properties of solid solutions $Lu_xY_{1-x}BO_3$ ($x = 0, 0.25, 0.50, 0.75, 1.00$) doped with Ce^{3+} or Eu^{3+} were investigated. It was found that the lattice parameters gradually decrease with an increase in the lutetium concentration in the solid solution. It was revealed that the solid solutions contain an additional calcite phase beginning with $x = 0.50$ for $Lu_xY_{1-x}BO_3 : Ce^{3+}$ and $x = 0.75$ for $Lu_xY_{1-x}BO_3 : Eu^{3+}$. The maximum content of the calcite phase in this case is less than 5 wt %.

The peaks observed in the luminescence spectra of the solid solutions are associated with the radiative recombination at the impurity ions. In the $Lu_xY_{1-x}BO_3 : Eu^{3+}$ solid solutions with intermediate concentrations x, the luminescence intensity increases under band-to-band excitation due to an increase in the efficiency of energy transfer to Eu^{3+} luminescence centers. This effect confirms the limited spatial separation of genetic electrons and holes in the solid solution. The formation of the calcite phase in the solid solutions leads to a significant decrease in the efficiency of energy transfer to the Eu^{3+} and Ce^{3+} luminescence centers. For the $Lu_xY_{1-x}BO_3 : Ce^{3+}$ solid solutions, it was found that, under high-energy excitation at 130 eV, apart from the main doublet of the Ce^{3+} luminescence with maxima at 380 and 420 nm, which is also observed under UV and VUV excitation, the luminescence spectrum contains an additional doublet with maxima at 315 and 344 nm. It was shown that the appearance of the additional doublet is caused by the formation of radiation-induced defects in the environment of the Ce^{3+} emitting ion. It was also established that, in the $Lu_xY_{1-x}BO_3 : Ce^{3+}$ solid solutions, the luminescence intensity gradually decreases with an increase in the concentration x. This effect is associated with a modification of the band structure in the region of the conduction band bottom, specifically with a decrease in the band gap due to the low-energy shift of the conduction band bottom. In this case, the Ce^{3+} $5d(1)$ level gradually shifts toward the conduction band bottom, which leads to a possible ionization of the Ce^{3+} excited state and, consequently, to a decrease in the Ce^{3+} luminescence intensity.

REFERENCES

1. B. V. Grinev, M. F. Dubovik, and A. V. Tolmachev, *Optical Single Crystals of Complex Oxide Compounds* (Institute for Single Crystals of the National Academy of Sciences of Ukraine, Khar'kov, 2002) [in Russian].

2. C. H. Kim, I. E. Kwon, C. H. Park, Y. J. Hwang, H. S. Bae, Y. B. Yu, C. H. Pyun, and G. Y. Hong, J. Alloys Compd. **311**, 33 (2000).

3. L. V. Ivanenko, Extended Abstract of Candidate's Dissertation (Stavropol State University, Stavropol, 2004).

4. F. Yang, S. Pan, and D. Ding, in *Abstracts of Papers of the Eleventh International Conference on Inorganic Scintillators and Their Applications, Giessen, Germany, September 12–16, 2011* (Giessen, 2011), O 4.22.

5. Y. Wu, D. Ding, S. Pan, F. Yang, and G. Ren, J. Alloys Compd. **509**, 366 (2010).

6. W. W. Moses, M. J. Weber, S. E. Derenzo, D. Perry, P. Berdahl, L. Schwarz, U. Sasum, and L. A. Boatner, in *Proceedings of the Fourth International Conference on Inorganic Scintillators and Their Applications, Shanghai, China, September 22–25, 1997* (Shanghai, 1997), p. 358.

7. B. I. Zadneprovski, V. V. Sosnovtsev, D. G. Permenov, A. A. Meotishvili, and G. I. Voronova, Tech. Phys. Lett. **35** (9), 815 (2009).

8. C. Mansuy, E. Tomasella, R. Mahiou, L. Gengembre, J. Grimblot, and J. M. Nedelec, Thin Solid Films **515**, 666 (2006).

9. S. Hatamoto, T. Yamazaki, J. Hasegawa, Y. Anzaiy, M. Katsurayama, and M. Oshika, J. Cryst. Growth **311**, 530 (2009).

10. G. Chadeyron-Bertrand, D. Boyer, C. Dujardin, C. Mansuy, and R. Mahiou, Nicl. Instrum. Methods Phys. Res., Sect. B **229**, 232 (2005).

11. A. N. Belsky, C. Dujardin, C. Pedrini, A. Petrosyan, W. Blanc, J. C. Gacon, E. Auffray, and P. Lecoq, in *Proceedings of the Fifth International Conference on Inorganic Scintillators and Their Applications, Moscow, Russia, August 16–20, 1999* (Moscow, 1999), p. 363.

12. A. N. Belsky, C. Dujardin, C. Pedrini, A. Petrosyan, W. Blanc, J. C. Gacon, E. Auffray, P. Lecoq, N. Garnier, and H. Canibano, IEEE Trans. Nucl. Sci. **48**, 1095 (2001).

13. Y. T. Wu, D. Z. Ding, S. K. Pan, F. Yang, and G. H. Ren, Cryst. Res. Technol. **46** (1), 48 (2011).

14. O. Sidletskiy, A. Belsky, A. Gektin, S. Neicheva, D. Kurtsev, V. Kononets, C. Dujardin, K. Lebbou, O. Zelenskaya, V. Tarasov, K. Belikov, and B. Grinyov, Cryst. Growth Des. **12**, 4411 (2012).

15. O. Sidletskiy, V. Kononets, K. Lebbou, S. Neicheva, O. Voloshina, V. Bondar, V. Baumer, K. Belikov, A. Gektin, B. Grinyov, and M. Joubert, Mater. Res. Bull. **47**, 3249 (2012).

16. G. Zimmerer, Radiat. Meas. **42**, 859 (2007).

17. A. E. Savon, Extended Abstract of Candidate's Dissertation (Moscow State University, Moscow, 2012).

18. C. U. S. Larsson, A. Beutler, O. Björneholm, F. Federmann, U. Hahn, A. Rieck, S. Verbin, and T. Möller, Nucl. Instrum. Methods Phys. Res., Sect. A **337**, 603 (1994).

19. J. Holsa, Inorg. Chim. Acta **139**, 257 (1987).

20. G. Blasse and B. C. Grabmaier, *Luminescent Materials* (Springer-Verlag, Berlin, 1994), p. 233.

21. S. Hachani, B. Moine, A. El-Akrmi, and M. Ferid, J. Lumin. **130**, 1774 (2010).

22. V. V. Mikhailin and A. N. Vasil'ev, *Introduction to the Solid State Spectroscopy* (Moscow State University, Moscow, 2010) [in Russian].

23. D. F. Shriver and P. W. Atkins, *Inorganic Chemistry,* Vol. 1: *Crystal Field Theory* (Oxford University Press, Oxford, 2001; Mir, Moscow, 2004), pp. 359−679.

24. M. Randic, J. Chem. Phys. **36**, 2094 (1962).

25. L. Zhang, C. Madej, C. Pedrini, C. Dujardin, J. C. Gacon, B. Moine, I. Kamenskikh, A. Belsky, D. A. Shaw, and M. A. Mac Donald, Radiat. Eff. Defects Solids **150**, 47 (1999).

26. R. E. Newnham, M. J. Redman, and R. S. Roth, J. Am. Ceram. Soc. **46**, 253 (1963).

27. W. F. Bradley, D. L. Graf, and R. S. Roth, Acta Crystallogr. **20**, 283 (1966).

28. G. Chadeyron, M. El-Ghozzi, R. Mahiou, A. Arbus, and J. C. Cousseins, J. Solid State Chem. **128**, 261 (1997).

29. M. Ren, J. H. Lin, Y. Dong, L. Q. Yang, M. Z. Su, and L. P. You, Chem. Mater. **11**, 1576 (1999).

30. J. H. Lin, D. Sheptyakov, Y. X. Wang, and P. Allenspach, Chem. Mater. **16**, 2418 (2004).

31. K. C. Mishra, B. G. DeBoer, P. C. Schmidt, I. Osterloh, M. Stephan, V. Eyert, and K. H. Johnson, Phys. Chem. **102**, 1772 (1998).

32. M. Balcerzyk, Z. Gontarz, M. Moszynski, and M. Kapusta, J. Lumin. **87−89**, 963 (2000).

33. D. A. Spassky, V. S. Levushkina, V. V. Mikhailin, B. I. Zadneprovski, and M. S. Tret'yakova, Phys. Solid State **55** (1), 150 (2013).

34. A. N. Belsky, O. Krachni, and V. V. Mikhailin, J. Phys.: Condens. Mater **5**, 9417 (1993).

35. M. Fasoli, A. Vedda, M. Nikl, C. Jiang, B. P. Uberuaga, D. A. Andersson, K. J. McClellan, and C. R. Stanek, Phys. Rev. B: Condens. Matter **84**, 081102 (2011).

Translated by O. Borovik-Romanova